Volume Changes Associated with CO Photolysis from Fully Reduced Bovine Heart Cytochrome aa_3†

Randy W. Larsen* and Tana Langley

Contribution from the Department of Chemistry, University of Hawaii at Manoa, 2545 The Mall, Honolulu, Hawaii 96822

Received August 17, 1998

Abstract: Volume changes associated with CO photodissociation from fully reduced cytochrome aa_3 have been determined using photoacoustic calorimetry (PAC). Analysis of PAC data reveals two intermediate steps in the photodissociation reaction with volume changes of +6.8 and +6.9 mL/mol occurring on time scales of <50 ns and ~1.5 μs, respectively (T = 22 °C). The value of ΔV for the fast process can be attributed to conformational dynamics associated with photoinduced transfer of CO from the high-potential heme a_3 to the high-potential Cu_B site, while the slower phase reaction occurs on a time scale consistent with the thermal dissociation of CO from Cu_B. It is speculated that these volume changes may be linked to movement of Glu-242 as part of a proton shuttle mechanism in heme/copper oxidases.

Introduction

Cytochrome *c* oxidase (CcO) represents a unique class of biomolecules that is capable of converting redox free energy into usable potential energy that is stored across a membrane barrier.[1−3] Thus, CcO operates as a molecular machine in a fashion similar to that of other protein-based transducers such as rhodopsin and bacteriorhodopsin.[4,5] Physiologically, CcO catalyzes the terminal step in the respiratory chain of a wide range of aerobic organisms including fungi, eukaryotic and prokaryotic bacteria, plants, and mammals. The preponderance of CcO containing mitochondria in critical mammalian tissue such as heart, liver, and brain exemplifies the enzyme's importance in maintaining health and well-being of higher organisms. Cytochrome *c* oxidase is a 13-subunit enzyme (three in most bacterial enzymes) that catalyzes the four-electron reduction of dioxygen to water according to the following reaction:

$$4\text{Cyt } c \text{ (red)} + 8H_m^+ + O_2 \rightarrow 4\text{Cyt } c \text{ (ox)} + 2H_2O + 4H_c^+$$

where H_m^+ and H_c^+ designate protons derived from the matrix side and cytosolic side of the inner-mitochondrial membrane, respectively. Cytochrome *c* oxidase carries out this catalytic process using five redox-active metal centers consisting of two heme A chromophores, three copper ions, and two additional metal sites (believed to play regulatory roles in catalysis) distributed between the largest three subunits of the enzyme. The reduction of dioxygen takes place at a binuclear cluster consisting of one heme A chromophore (designated cytochrome a_3) and one copper ion (designated Cu_B). The two remaining metal centers (designated cytochrome *a* and a binuclear Cu_A) have reduction potentials near that of cytochrome *c* and mediate electron flow from ferrocytochrome *c* to the binuclear center.

The recent crystal structures of the bovine enzyme as well as that from *Paracoccus denitrificans* coupled with site directed mutagenisis studies with *Rhodobacter spheroidies* have shed considerable light onto the mechanism of redox-linked proton translocation.[6−10] A picture is now emerging in which subunit I of the enzyme contains a number of channels capable of transporting protons, oxygen, and water. In addition, mutagenisis studies indicate independent pathways for protons actively transported to the cytosol (from the matrix) and protons consumed for dioxygen reduction.[6,10] In all cases, conformational dynamics are required to form these channels, consistent with previous models which suggest that the enzyme complex must undergo an ordered sequence of conformational transitions to complete its catalytic cycle.[2,11,12] The binding of dioxygen to the two-electron-reduced binuclear center appears to induce a conformational change in the enzyme that "activates" the proton pump cycle.[2] Additional conformational changes are then required to modulate ("gate") both electron and proton transfer

* To whom correspondence should be addressed.

†A preliminary report of this work was presented at the 1998 Biophysical Society meeting, Kansas City, MO, February 22−26, 1998.

(1) Papa, S. *Biochim. Biophys. Acta* **1976**, *456*, 39−84.

(2) Musser, S. M.; Stowell, M. H. B.; Chan, S. I. *Advances in Enzymology and Related Areas of Molecular Biology*; Meister, A., Ed.; Wiley and Sons: New York, 1995.

(3) Wikstrom, M.; Krab, K.; Saraste, M. *Cytochrome Oxidase. A Synthesis*; Academic Press: London, 1981.

(4) Nathans, J. *Biochemistry* **1992**, *31*, 4923−4931.

(5) Birge, R. R. *Ann. Rev. Phys. Chem.* **1990**, *41*, 683−733.

(6) Fetter, J. R.; Qian, J.; Shapleigh, J.; Thomas, J. W.; Garcia-Horsman, A.; Schmidt, E.; Hosler, J.; Babcock, G. T.; Gennis, R. B.; Ferguson-Miller, S. *Proc. Natl. Acad. Sci. U.S.A.* **1995**, *92*, 1604−1608.

(7) Hosler, J. P.; Shapleigh, J. P.; Mitchell, D. M.; Kim, Y.; Pressler, M. A.; Georgiou, C.; Babcock, G. T.; Alben, J. O.; Ferguson-Miller, S.; Gennis, R. B. *Biochemistry* **1996**, *35*, 10776−10783.

(8) Hosler, J. P.; Ferguson-Miller, S.; Calhoun, M. W.; Thomas, J. W.; Hill, J.; Lemieux, L.; Ma, J.; Georgiou, C.; Fetter, J.; Shapleigh, J.; Tecklenburg, M. M. J.; Babcock, G. T.; Gennis, R. B. *J. Bioenerg. Biomembr.* **1993**, *25*, 121−136.

(9) Iwata, S.; Ostermeier, C.; Ludwig, B.; Michel, H. *Nature* **1995**, *376*, 660−669.

(10) (a) Tsukihara, T.; Aoyama, H.; Yamashita, E.; Tomizaki, T.; Yamaguchi, H.; Shinzawa-Itoh, K.; Nakashima, R.; Yaono, R.; Yoshikawa, S. *Science* **1995**, *269*, 1069−1074. (b) Tsukihara, T.; Aoyama, H.; Yamashita, E.; Tomizaki, T.; Yamaguchi, H.; Shinzawa-Itoh, K.; Nakashima, R.; Yaono, R.; Yoshikawa, S. *Science* **1995**, *269*, 1069−1074.

(11) Gelles, J.; Blair, D. F.; Chan, S. I. *Biochim. Biophys. Acta* **1986**, *853*.

(12) Larsen, R. W.; Pan, L. P.; Musser, S. M.; Li, Z.; Chan, S. I. *Proc. Natl. Acad. Sci. U.S.A. 89*, 723−727.

10.1021/ja9829517 CCC: $18.00
Published on Web 04/27/1999

as well as to physically transport the protons through the enzyme. Such conformational changes are required to ensure favorable kinetics for proton translocation and must be linked to a change in oxidation state of one or more of the four redox-active metal sites contained within the enzyme complex. These conformational changes are likely to occur *transiently* during the catalytic cycle of the enzyme and in some cases may represent the rate-limiting step in the overall reaction.

There is now considerable evidence for steady-state conformational changes in CcO after ligand binding and electron transfer. Recent studies of CcO involving high-pressure optical spectroscopy of steady-state enzyme turnover have revealed large volume changes associated with conversion between various intermediates.[13−16] Volume changes as large as 76 mL/mol have been observed and attributed to the uptake of water molecules by the enzyme.[14,15] In addition, we have observed conformational differences between P-state and F-state enzymes consistent with previous fluorescence experiments.[17,18] Although these observations shed some light on the relationship between conformational dynamics and proton transport in CcO, no systematic conformational study on physiological time scales have been undertaken.

Photoacoustic calorimetry (PAC) is proving to be a powerful technique for determining the magnitude and time scale of conformational changes as well as reaction thermodynamics in proteins and enzymes. For example, PAC has been previously employed to investigate conformational changes associated with ligand photolysis from hemoglobin, myoglobin, and cytochrome P450 as well as the catalytic cycle of rhodopsin and bacteriorhodopsin.[20−23] The physical principle behind PAC is that photoexcited molecules dissipate excess energy via vibrational relaxation to the ground state accompanied by thermal heating of the surrounding solvent. For solvents such as water, this causes rapid volume expansion resulting in an acoustic wave that can be detected with a sensitive piezoelectric crystal based microphone. In addition, volume changes in the system of interest, resulting from a photoinitiated reaction also contribute to the acoustic wave. After normalizing the signal acoustic wave with that of an appropriate reference compound (one that is nonfluorescent and does not undergo any photochemistry) the following expression is obtained:

$$\phi E_{h\nu} = (S/S_{\mathrm{ref}})E_{h\nu} = Q + \{\Delta V_{\mathrm{con}}/F(T)\} \qquad \text{(I)}$$

where $F(T) = (\beta/C_p\rho)$ (β = thermal expansion coefficient of water in K^{-1}, C_p = heat capacity in cal/g-deg-mol, and ρ = density in g/mL), Q is the amount of heat released to the solvent after photolysis, and $E_{h\nu}$ is the energy of the excitation photon. A plot of normalized photoacoustic amplitude (ϕ) versus $1/F(T)$ gives a straight line with a slope equal to ΔV_{con} associated with a change in conformation and an intercept equal to the heat evolved (Q). Subtracting Q from $E_{h\nu}$ gives ΔH for the reaction.

For reactions which involve multiple steps with time scales between 10 ns and ~5 μs (depending on transducer type), the individual contributions of ΔV_{con} and Q for each step to the total amplitude can be resolved. For a two-step reaction of the type

$$\mathrm{A} \xrightarrow{k_1} \mathrm{B} \xrightarrow{k_2} \mathrm{C}$$

the observed time-dependent acoustic signal results from a convolution of a time-dependent volume source, $H(t)$, with an instrument response function, $T(t)$:

$$E(t)_{\mathrm{obs}} = H(t)\ T(t) \qquad \text{(II)}$$

$$H(t) = \phi_1 \exp(-t/\tau_1) + [\phi_2 k_2/(k_2 - k_1)][\exp(-t/\tau_1) - \exp(-t/\tau_2)] \qquad \text{(III)}$$

with $k_i = 1/\tau_i$. Deconvolution of the signal involves estimating the parameters in $H(t)$ and convoluting the test $H(t)$ with $T(t)$ obtained from an appropriate calibration compound. The convoluted waveform E_{calc} is compared with $E(t)_{\mathrm{obs}}$, and the parameters in $H(t)$ are varied until a reasonable fit is obtained.

We have recently utilized PAC to probe conformational dynamics associated with photolysis of an COFe(II)PPIX/micelle model system and fully reduced CO-bound cytochrome bo_3 from *E. coli*.[19] Analysis of PAC of the cytochrome bo_3 system revealed an enthalpy for CO photodissociation of +22.7 ± 6.8 kcal/mol and an accompanying volume decrease of 5.1 ± 0.9 mL/mol. The data further indicate that the enthalpy and volume changes occur on a time scale of <50 ns. Thus, these values represent ΔH and ΔV for the photoinduced transfer of CO from the high-potential heme o_3 to the high-potential Cu_B site. The observed volume and enthalpy changes are consistent with a significant protein conformational change associated with this reaction. In addition, no transient species are observed between 50 ns and ~5 μs, confirming that the thermal dissociation of CO from Cu_B occurs on time scales of >5 μs. We have extended this work to examine conformational changes associated with photolysis of the fully reduced CO-bound CcO from bovine heart. The results demonstrate important differences in the conformational dynamics of ligand binding in heme/copper oxidases.

Materials and Methods

Bovine CcO was purified as described previously.[24] Sodium dithionite (Aldrich) and CO (Matheson) were used as received. Samples for PAC were prepared by diluting the CcO stock solution (~250 μM) to ~100 μM CcO in 100 mM HEPES buffer/0.1% lauryl maltoside (pH 7.5) in a 1 cm path length quartz cuvette (total volume 0.5 mL). The cuvette was then sealed with a septum cap. The sample was then purged with Ar for 30 min (the sample was placed on ice during the purging) followed by the addition of sodium dithionite. After full reduction of the enzyme is complete (as judged by optical absorption), the sample was purged for an additional 10 min with CO.

PAC signals associated with CO photolysis were obtained by placing a 1 × 1 cm quartz optical cuvette containing the sample on the center of our photoacoustic detector. Contact between the cuvette and the detector is facilitated by a thin layer of vacuum grease. The acoustic detector is based upon a Transducer Products PZT-2H piezoelectric

(13) Kornblatt, J. A.; Hoa, G. H. B.; Heremans, K. *Biochemistry* **1988**, *27*, 5122−5128.
(14) Kornblatt, J. A.; Hoa, G. H. B. *Biochemistry* **1990**, *29*, 9370−9376.
(15) Kornbaltt, J. A.; Kornblatt, M. J. *Biochim. Biophys. Acta* **1992**, *1099*, 182−184.
(16) Kornblatt, J. A.; Kornblatt, M. J.; Kahn, P. C. *Biophys. J.* **1998**, *75*, 435.
(17) Larsen, R. W. *FEBS Lett.* **1994**, *352*, 365−368.
(18) Niu, S. N.; Larsen, R. W. *J. Biochem., Mol. Biol., Biophys.* **1998**, *1*, 287−293.
(19) (a) Larsen, R. W. *Inorg. Chim. Acta*, in press. (b) Larsen, R. W.; Osborne, J.; Langley, T.; Gennis, R. B. *J. Am. Chem. Soc.*. **1998**, *120*, 8887−8888.
(20) (a) Peters, K. S.; Watson, T.; Logan, T. *J. Am. Chem. Soc.* **1992**, *114*, 4276−4278. (b) Peters, K. S.; Watson, T.; Logan, T. *J. Am. Chem. Soc.* **1992**, *114*, 4276−4278.
(21) Di Primo, C.; Hoa, G. H. B.; Deprez, E.; Douzou, P.; Sligar, S. G. *Biochemistry* **1993**, *32*, 3671−3676.
(22) Westrick, J. A.; Peters, K. S.; Ropp, J. D.; Sligar, S. G. *Biochemistry* **1990**, *29*, 6741−6746.
(23) Schulenberg, P. J.; Rohr, M.; Gartner, W.; Braslavsky, S. E. *Biophys. J.* **1994**, *66*, 838−843.
(24) Niu, S.-N. Dissertation, University of Hawaii at Manoa, 1997.

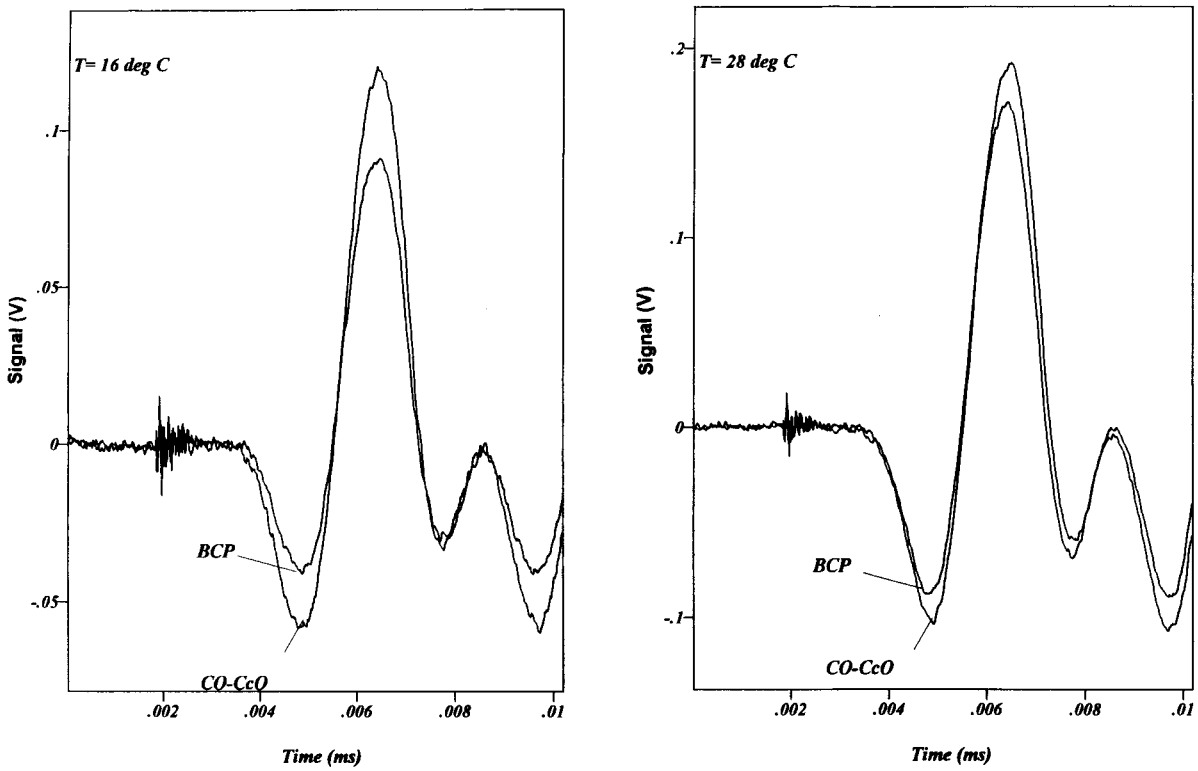

Figure 1. Overlay of the photoacoustic waves for bromocresol purple and CO−CcO at 28 °C (left panel) and 18 °C (right panel). Sample concentrations are 100 μM for COCcO and 1 mM BCP (100 mM Tris/0.1% laurylmaltoside, pH 7.5). The excitation wavelength is 532 nm with an average power of ~80 μJ/pulse.

crystal (2 mm in diameter) that is silvered on each end. The crystal is housed in an aluminum case such that one side of the crystal makes contact with the top of the cylinder. The crystal is held in place by a steel spring which also serves as the signal carrier to a BNC connector. Sound waves generated by pulsed laser photolysis (Continuum SureLite I frequency doubled Nd:YAG laser, 7ns, ~80 μJ/pulse) of the sample result in compression of the crystal and generation of a voltage between the two sides that is amplified and recorded using a 200 MHz transient digitizer (Tektronix RTD710A). The trigger for the digitizer is supplied by a photodiode sensing the laser pulse. This ensures correct timing of the data collection. With our current detection system, volume changes occurring on time scales ranging from 50 ns to ~5 μs can be observed.

The values for C_p, ρ, and β as a function of temperature (and therefore $1/F(T)$) are known for water.[25] The corresponding values of $F(T)$ for the detergent/buffer system to be used (100 mM HEPES buffer/0.1% lauryl maltoside) were determined by comparing acoustic signal amplitudes of the calibration compound BCP as a function of temperature in the detergent/buffer vs those for BCP in water. From the relationship

$$(\beta/C_p\rho)_{buffer} = (S_{buffer}/S_{water})(\beta/C_p\rho)_{water} \qquad \text{(IV)}$$

the values of $(\beta/C_p\rho)_{buffer}$ as a function of temperature can be found by measuring the signal amplitude of the calibration compound in water and buffer as a function of temperature. This equation holds providing the compressibilty factor between the two solvents is the same. The compressibilty factor is expressed as ρv_a^2 with v_a being the velocity of sound in the given solvent.[26] This value is obtained from the arrival time of the acoustic wave to the detector. In the present case, $v_a^{water} = v_a^{buffer}$ within experimental error, thus indicating similar compressibilities.

Results

Figure 1 displays overlays of the acoustic wave for the reference compound bromocresol purple (BCP) and CO−CcO at 16 °C (left panel) and 28 °C (right panel). The acoustics waves for CO−CcO show a shift in phase, relative to the reference compound. This indicates that a process or processes occur(s) on time scales between 50 ns and 5 μs. Deconvolution of the acoustic wave for CO−CcO using simplex software developed in our laboratory reveals two exponential decays associated with the CO−CcO acoustic signal. Figure 2 displays a representative example of the deconvolution. The first decay occurs with a lifetime shorter than the detection limit of our instrument (i.e., <50 ns) while the second process exhibits a lifetime of 1.3 μs at 22 °C. Plots of $E_{h\nu}\phi_1$ and $E_{h\nu}\phi_2$ vs $C_p\rho/\beta$ (Figure 3) (ϕ_1 and ϕ_2 were obtained from eqs II and III) for the photolysis of CO from fully reduced CcO give volume increases of +6.8 mL/mol (ΔV_1) and +6.9 mL/mol for the fast and slow phases, respectively. (The slope obtained from the slow phase data actually represents the *total* volume change for the ligand dissociation reaction, i.e., ΔV_{1+2}. The volume change for the slow phase is then obtained by subtracting the fast phase volume change from the *total* volume change, $\Delta V_2 = \Delta V_{1+2} - \Delta V_1$). Comparison of volume changes associated with CO photolysis from various heme proteins is given in Table 1. The values for ΔH have not yet been determined since the absorbance contribution for cytochrome *a* and cytochrome a_3 at 532 nm (excitation wavelength) are not known.[19] We are currently working to obtain these values using heme *a* reconstituted myoglobin to estimate the absorbance contributions.

Discussion

Time-resolved optical and vibrational spectroscopies have revealed a mechanism for CO dissociation from CcO in which CO (photodissociated from heme a_3) binds first to the nearby Cu_B site ($t_{1/2}$ 1ps <) followed by dissociation and diffusion into

(25) *CRC Handbook of Chemistry and Physics*, 59th ed.; CRC Press: Boca Raton, FL, 1978.

(26) Churio, M. S.; Angermund, K. P.; Braslavsky, S. E. *J. Phys. Chem.* **1994**, *98*, 1776−1782.

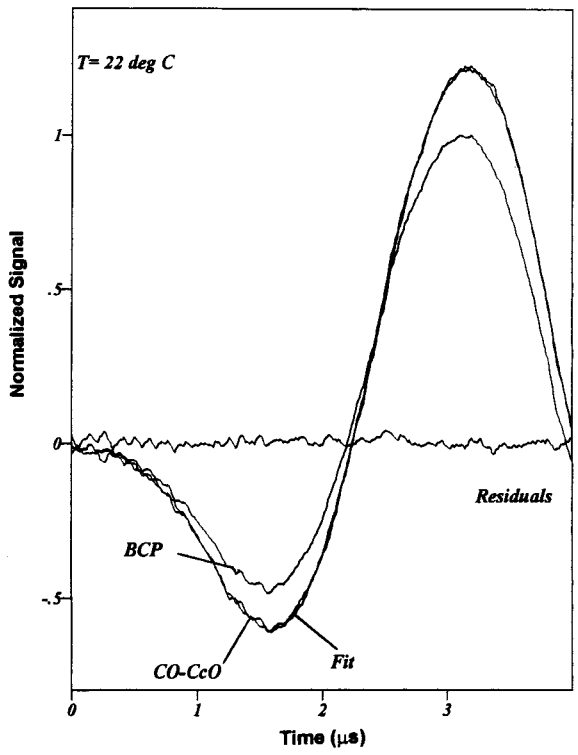

Figure 2. Acoustic waveform of bromocresol purple (reference compound), CO−CcO (sample wave), CO−CcO fitted to two exponential decays (fitted wave), and residuals of the fit. Deconvolution was performed using the Simplex-based parameter optimization program developed in our laboratory. The lifetimes for the two phases are <50 ns (fast phase, ϕ_1) and ~1.5 μs (slow phase, ϕ_2) at $T = 22$ °C. The χ^2 value for the fit is 0.025.

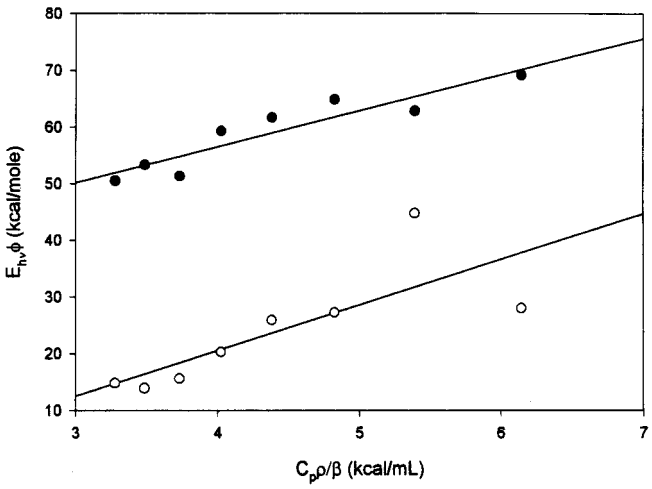

Figure 3. Plot of $E_{h\nu}\phi_1$ (closed circles) and $E_{h\nu}\phi_2$ (open circles) (kcal/mol) vs $C_p\rho/\beta$ (kcal/mL). The values for ϕ_1 and ϕ_2 were obtained for the two exponential decays derived from the Simplex deconvolution.

the bulk solvent ($t_{1/2} \sim 1-3$ μs) (see Figure 4).[27] Of particular interest is the fact that formation of the Cu_B−CO complex occurs at a rate 100-fold slower than that expected for a diffusion-controlled reaction, suggesting that the protein can limit access to the heme/copper active site. The volume changes observed after CO photolysis from fully reduced CcO occur on the same time scale as CO dissociation from cytochrome a_3/binding to Cu_B (the fast phase component of the acoustic wave)

Table 1. Volume Changes and Reaction Enthalpies for CO Photodissociation from Selected Proteins

protein	ΔV (mL/mol)	ΔH (kcal/mol)	ref
CO−Cyt P450[a]	+1.8	2.2	21
CO−Mb[b]	−9/+5.8	0.8/9.9	20a
CO−HbA[c]	+23.5	18	20b
CO−Cbo	−5.1	22.7	19
CO−CcO[d]	+6.8/+6.9	−	this work

[a] Camphor free. [b] Values before slash refer to formation of an intermediate species, while values after slash refer to the decay of this intermediate. [c] For the reaction $(CO)_4Hb \rightarrow (CO)_3Hb + CO$. [d] Value before slash refers to the <50 ns process, while value after slash is for the 1.5 μs process.

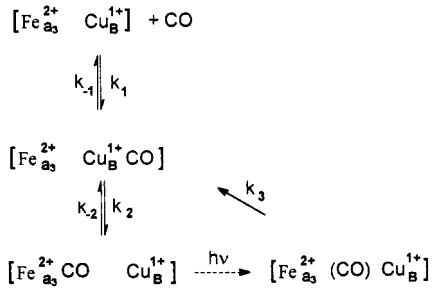

Figure 4. Mechanism of CO binding to heme/copper terminal oxidases. For bovine CcO, $k_{-1} = 6.5 \times 10^5$ s^{-1}, $k_1 = 5.9 \times 10^7$ M^{-1} s^{-1}, $k_2 = 1.1 \times 10^3$ s^{-1}, $k_{-2} = 0.023$ s^{-1}, $k_3 > 1 \times 10^9$ s^{-1} (from ref 26).

and thermal dissociation of CO from Cu_B (slow phase component of the acoustic wave). Thus, it is likely that these volume changes represent a protein conformational response as a result of "local" events occurring at the binuclear center (since PAC samples *overall* volume changes). The dissociation of CO from cytochrome a_3 induces structural changes to the heme group itself including doming of the porphyrin ring, displacement of the heme iron out of the plane of the porphyrin ring, and a change in spin state of the heme iron. High-pressure studies have revealed a volume change associated with porphyrin spin state changes to be on the order of +10 mL/mol (heme Fe low-spin to high-spin transition).[28,29] The binding of CO to Cu_B may also contribute to the initial volume increase. Previous studies have suggested that a ligand associated with Cu_B is displaced upon CO binding to the metal.[26] Within this mechanism the displaced ligand (displaced by CO binding to Cu_B) binds to the iron of cytochrome a_3. Time-resolved magnetic circular dichroism data further indicate that cytochrome a_3 remains high spin after photolysis. Such structural changes associated with the Cu_B site upon CO binding would also make a significant contribution to the observed volume change.

The volume expansion ($\Delta V_2 = +6.8$ mL/mol) observed for the slower process (with a time constant similar to the thermal dissociation of CO from Cu_B) may be attributed to perturbation of the protein upon ligand release from the Cu_B site.[27] This process should have a volume change equal in magnitude but opposite in sign to that associated with CO binding to Cu_B. Therefore, if the fast phase volume change can be thought of as the sum of volume changes associated with heme distortions as well as CO binding to Cu_B (i.e., $\Delta V_1 = \Delta V_{heme} + \Delta V_{Cu+CO}$), then the heme contributions would be on the order of −7 mL/mol (i.e., $\Delta V_1 - (-\Delta V_2)$). It should also be pointed out that the time scale for this volume change is distinct from the Fe-His relaxation rate determined using resonance Raman ($t_{1/2} \sim 10$ μs), indicating that the observed conformational change is

(27) Einarsdottir, O.; Dyer, B. R.; Lemon, D. D.; Killough, P. M.; Hubig, S. M.; Atherton, S. J.; Lopez-Garriga, J. J.; Palmer, G.; Woodruff, W. H. *Biochemistry* **1993**, *32*, 12013−12024.

(28) van Eldik, R.; Asano, le Noble, W. J. *Chem. Rev.* **1989**, *89*, 549.

(29) Taube, D. J.; Projahn, H.-D.; van Eldik, R.; Magde, D.; Traylor, T. G. *J. Am. Chem. Soc.* **1990**, *112*, 6880−6886.

not associated with Fe−His relaxation. We speculate that the observed conformational change may be a protein response to changes in the coordination sphere of Cu_B.

Coupling between ligand binding to the binuclear center and proton translocation has recently been suggested. Studies utilizing FTIR spectroscopy have shown that CO binding to the Cu_B site of *E. coli* cytochrome bo_3 perturbs Glu-286, which is located at the end of a putative proton channel (the "D" channel).[30−32] Site-directed mutagenisis of this residue in either *E. coli* or *R. spheroidies* results in diminished activity and no proton pumping activity. Interestingly, Glu-286 is not directly linked to Cu_B or to any ligands of Cu_B. However, a bridge between Cu_B and Glu-286 could be facilitated by several water molecules providing proton conduction to the binuclear center. It has also been suggested that Glu-286 can toggle between different conformations, forming a gate for proton input and output to the binuclear center. Photoacoustic results for CO photolysis from fully reduced cytochrome bo_3 from *E. coli* demonstrate a volume contraction associated with CO binding to Cu_B. It was argued that a protein conformational change results in a volume decrease and that this conformational change may be responsible for the perturbation of Glu-286. This residue is conserved in bovine heart CcO as Glu-242. The recent crystal structure of fully oxidized bovine heart CcO reveals connectivity between Cu_B and Glu-242 via Pro-241 and His-240, with His-240 being one of the ligands for Cu_B.[9,10] Interestingly, the conformational response of CcO to the binding of CO to Cu_B is quite distinct (−5 mL/mol for cytochrome bo_3 vs +6.8 mL/mol for CcO) from that of cytochrome bo_3, indicating differences in coupling between the binuclear center and Glu-242/286 within heme/copper oxidases.

Both spectroscopic data and the results of the current work indicate a structural change in the protein associated with the transfer of CO from the heme Fe to Cu_B and the accompanying thermal release of CO from Cu_B. It is not known whether these structural changes are related to the differences in the kinetics of CO recombination in comparison with the other heme/copper oxidases or whether this phenomenon is typical of this class of enzyme. Such protein conformational changes may be responsible for "gating" ligand access to the binuclear center or may be related to the proton pumping mechanism. We are currently investigating these possibilities.

Acknowledgment. The authors acknowledge an American Heart Association Grant-in-Aid (HIGS-11-97) for support of this work. We also thank Prof. Robert B. Gennis (School of Chemical Sciences, University of Illinois, Urbana) for invaluable discussion during the course of this work.

JA9829517

(30) Tsubaki, M.; Hori, H.; Mogi, T. *Febs Lett.* **1997**, *416*, 247−250.
(31) Puustinen, A.; Bailey, J. A.; Dyer, B. R.; Mecklenburg, S. L.; Wikstrom, M.; Woodruff, W. H. *Biochemistry* **1997**, *36*, 13195−13200.
(32) Adelroth, P.; Ek, M. S.; Mitchell, D. M.; Gennis, R. B.; Brzezinski, P. *Biochemistry* **1997**, *36*, 13824−13829.